

Familial Cavernous Malformation

Published on 22.03.2021

DOI: 10.35100/eurorad/case.17180

ISSN: 1563-4086

Section: Neuroradiology

Area of Interest: CNS

Imaging Technique: MR

Case Type: Clinical Cases

Authors: Jesper Dierickx^{1,2}, Filip Vanhoenacker^{1,2,3}

Patient: 68 years, female

Clinical History:

A 68-year-old woman was referred for an MRI examination of the spine. She had no neurological symptoms or back pain.

She has a prior MRI examination of the brain and was known to have had multifocal brain lesions (further history withheld). The spine MRI was performed to screen for spinal lesions.

Imaging Findings:

On spine MRI, sagittal T1-WI and T2-WI (Fig. 1) show a solitary, punctate hyperintense focus on the medulla at the thoracic vertebra 11 levels (Th11). Axial T2-WI images at the Th11 level with fat saturation (Fig. 2) confirm the punctate, hyperintense lesion at the right anterolateral grey-white matter junction of the medulla. Blooming is present on sagittal gradient-echo T2-WI (Fig. 3), demonstrating a more prominent appearance and strong signal drop.

On brain MRI, axial T2-WI (Fig. 4a) and FLAIR images (Fig. 4b) show several supratentorial cortical and subcortical lesions. The lesion's centre has a reticular, mixed hypo- and hyper signal on both T2-WI and T1-WI (Fig. 5), with a hypo-intense rim on T2-WI. On susceptibility-weighted imaging (SWI), these lesions show blooming effect, with a more prominent hypo-intense signal (Fig. 6). Several additional hypo-intense, punctate subcortical lesions are present on SWI, but not visible on other sequences.

Discussion:

Cavernous malformation (CM) consists of slow flow, dilated capillary vessels with endothelial delineation [1]. CM has a reported prevalence of 0.4-0.6%. Spinal manifestations account for 5% of all CMs [2]. It has an idiopathic, sporadic form and a familial form [1]. Familial CM (FCM) has an autosomal dominant inheritance pattern with variable penetrance. Three related gene loci have been identified [3,4]. Genetic proof was not available in this patient. The patient has one sibling with FCM and with a history of spinal and intracranial haemorrhages. In the presence of multiple CMs, or one CM and at least one family member with CM, the FCM diagnosis can be made [1]. In familial forms, multifocality and progressively appearing new lesions are frequent [3,5]. CM occurs most frequently in supratentorial, lobar regions [3]. Patients with intracranial lesions usually present with seizure, headache or focal neurologic deficit. Patients with spinal lesions may demonstrate acute, stepwise or slow, progressive neurologic deterioration, including motoric or sensory disturbances, pain or urinary or bowel dysfunction. Asymptomatic spinal lesions are rare (0.9%) [2].

MRI is the preferred imaging modality with the highest sensitivity and specificity. Large CMs exhibit reticular, mixed hypo- and hyperintense signal in the lesion's centre on T1- and T2-WI, described as a "popcorn-like" pattern, reflecting old and recent haemorrhages [6]. Perilesional oedema and mass effect are typically absent in uncomplicated cases [3,6]. Hemosiderin causes a hypo-intense rim, visible on T2-WI and gradient-echo sequences. Smaller CMs are punctate and hypo-intense on T2-WI. On gradient-echo sequences, CMs are bigger due to the susceptibility of hemosiderin deposition ("blooming effect") [3]. SWI may display lesions not visible on other sequences [7]. Spine MRI shows similar "popcorn-like" lesions with hypo-intense rim on T2-WI and blooming effect on susceptibility sequences [8].

The differential diagnosis of brain involvement includes disorders with microbleeds such as diffuse axonal injury (DAI) or cerebral amyloid angiopathy (CAA). These microbleeds may have a similar, punctate, hypo-intense signal compared to small CMs. In contrast to FCM, "popcorn-like" morphology is absent in these disorders [9]. Hemorrhagic metastases may occur in melanoma, renal cell carcinoma, lung and thyroid carcinomas [9]. Radiation-induced CMs may occur several years following radiation therapy [9]. Spinal CMs should be differentiated from intramedullary tuberculoma. Tuberculomas don't show blooming effect, due to the absence of blood products [10].

In patients with FCM, susceptibility sequences are useful to detect spinal CM and differentiate them from other lesions.

Written informed patient consent for publication has been obtained.

Differential Diagnosis List: Familial cavernous malformation, Axonal injury, Radiation-induced microbleed, Hemorrhagic metastasis, Familial amyloid angiopathy, Intramedullary tuberculous granuloma

Final Diagnosis: Familial cavernous malformation

References:

- Morrison L, Akers A. (2019) Cerebral Cavernous Malformation , Familial. In: Adam M, Ardinger H, Pagon R, Wallace S, Bean L, Stephens K, Amemiya A. GeneReviews. Seattle (WA): University of Washington, Seattle (PMID: [20301470](#))
- Clark AJ, Wang DD, Lawton MT. (2017) Spinal cavernous malformations. In: Spetzler R, Moon K, Almefty R. Handbook of Clinical Neurology. Elsevier B.V. 143:303-308 (PMID: [28552154](#))
- Biscoito L. (2019) Intracranial Vascular Malformations. In: Barkhof F, Jager R, Thurnher M, Rovira Canellas A. Clinical Neuroradiology. Springer, Cham (DOI: 10.1007/978-3-319-61423-6_79-1).
- Ene C, Kaul A, Kim L. (2017) Natural history of cerebral cavernous malformations. In: Spetzler R, Moon K, Almefty R. Handbook of Clinical Neurology. Elsevier B.V. 143:227-232 (PMID: [28552144](#))
- Batra S, Lin D, Recinos P, Zhang J, Rigamonti D. (2009) Cavernous malformations: Natural history, diagnosis and treatment. Nat Rev Neurol. 5(12):659–70 (PMID: [19953116](#)).
- Wang K, Idowu O, Lin D. (2017) Radiology and imaging for cavernous malformations. In: Spetzler R, Moon K, Almefty R. Handbook of Clinical Neurology. Elsevier B.V. 143:249–266. (PMID: [28552147](#))
- Zafar A, Quadri S, Farooqui M, Ikram A, Robinson M, Hart B, Mabray M, Vigil C, Tang A, Kahn M, Yonas H, Lawton M, Kim H, Morrison L. (2019) Familial Cerebral Cavernous Malformations. Stroke. 50(5):1294–1301 (PMID: [30909834](#))
- Peckham ME, Hutchins TA. (2019) Imaging of Vascular Disorders of the Spine. Radiol Clin North Am. 57(2):307–318 (PMID: [30709472](#))
- Haller S, Vernooij M, Kuijjer J, Larsson E-M, Jäger HR, Barkhof F. (2018) Cerebral Microbleeds: Imaging and Clinical Significance. Radiology. 287(1):11–28 (PMID: [29558307](#))

Altinkaya N, Alkan O. (2015) Magnetic Resonance Imaging of Unusual Intramedullary Spinal Cord Lesions. *J Clin Anal Med.* 6(suppl 6):890–895 (DOI:10.4328/jcam.3518).

Figure 1

a



Description: Sagittal T1-WI demonstrate a punctate, hyperintense focus in the anterior part of the medulla (white arrow). **Origin:** © Department of Radiology, Algemeen Ziekenhuis Sint-Maarten, Mechelen, Belgium, 2020

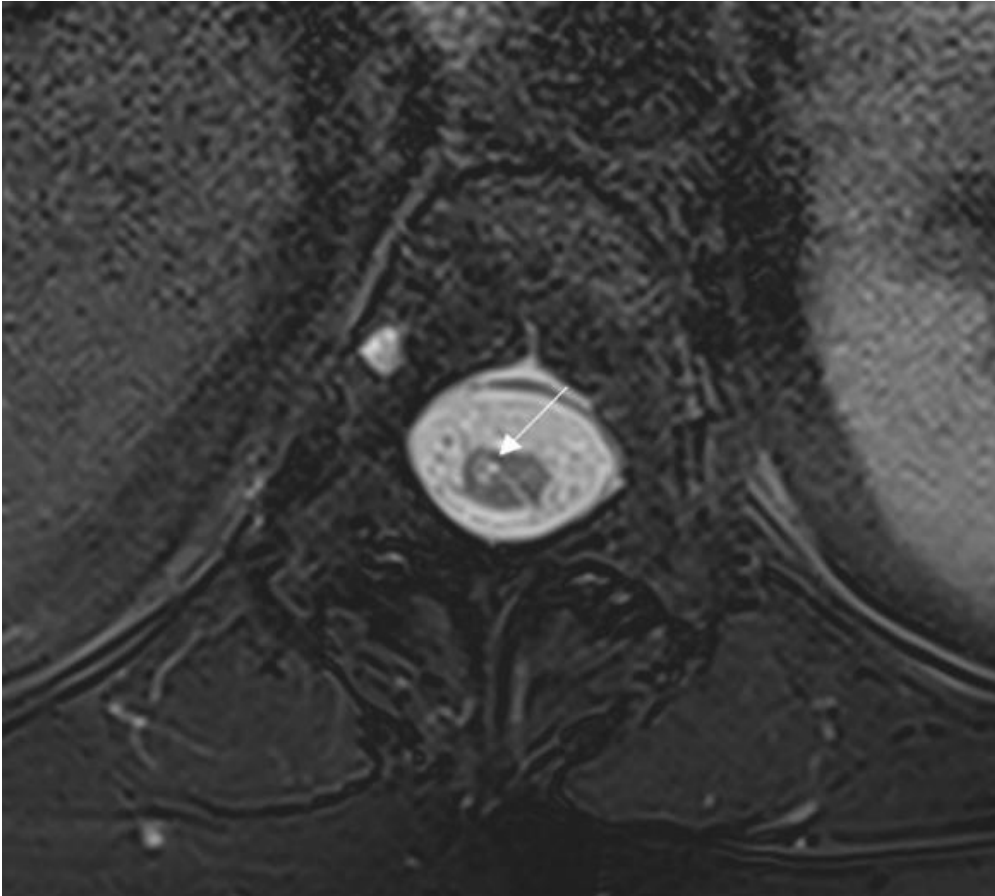
b



Description: Sagittal T2-WI demonstrate a punctate, hyperintense focus in the anterior part of the medulla (white arrow). Oedema is absent. **Origin:** © Department of Radiology, Algemeen Ziekenhuis Sint-Maarten, Mechelen, Belgium, 2020

Figure 2

a



Description: Axial T2-WI with fat saturation confirm a punctate, hyperintense lesion in the right anterolateral part of the medulla, near the gray-white matter junction (white arrow). **Origin:** © Department of Radiology, Algemeen Ziekenhuis Sint-Maarten, Mechelen, Belgium, 2020

Figure 3

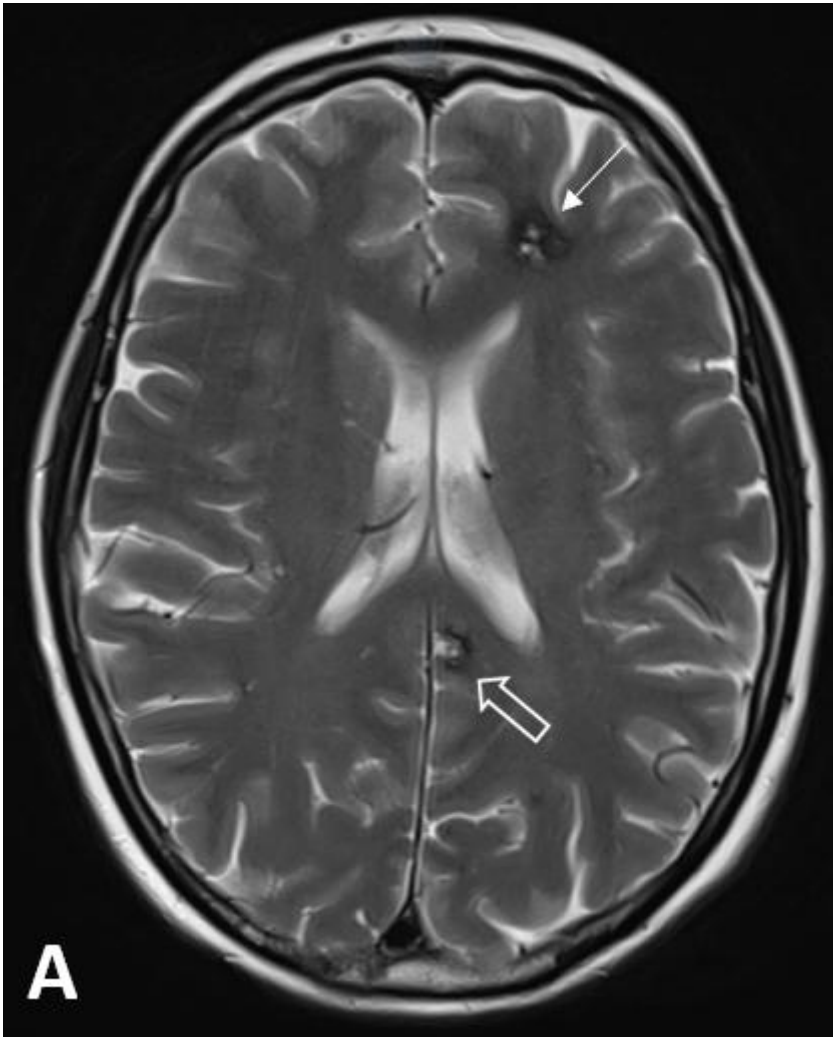
a



Description: Sagittal gradient echo T2-WI demonstrate blooming effect in the intramedullary lesion (white arrow). **Origin:** © Department of Radiology, Algemeen Ziekenhuis Sint-Maarten, Mechelen, Belgium, 2020

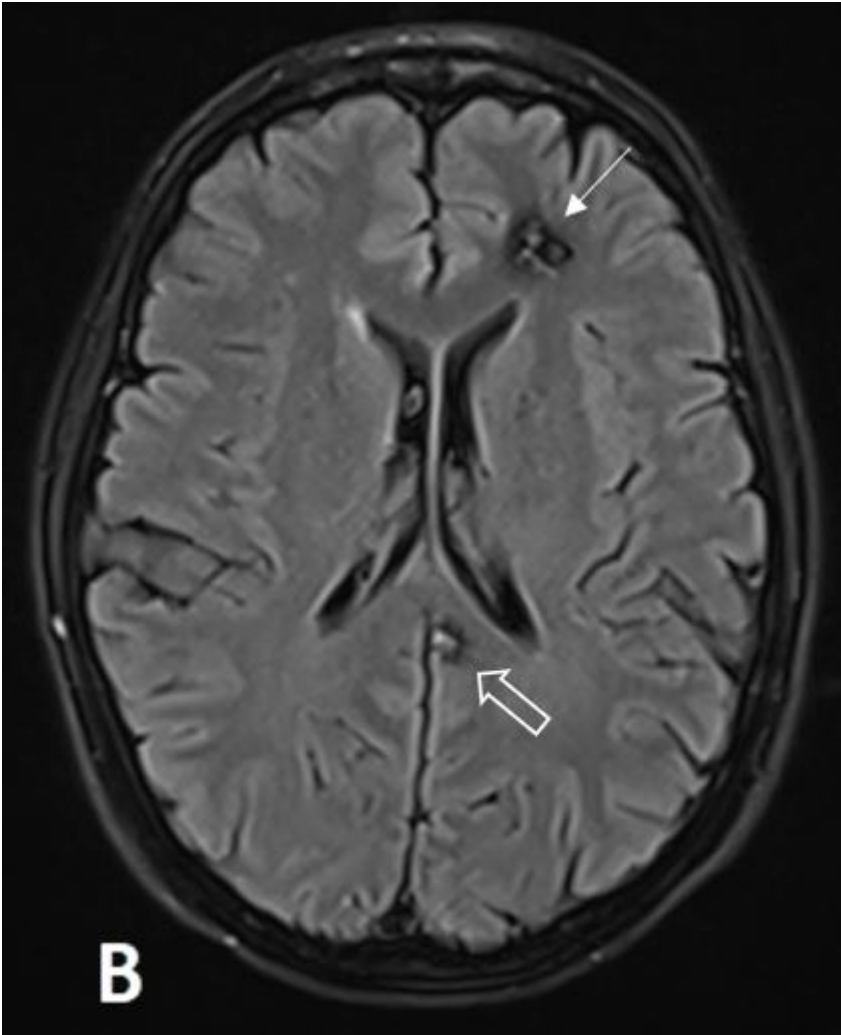
Figure 4

a



Description: Axial T2-WI demonstrate a subcortical-located lesion in the left frontal lobe (white arrow) and a parafalcine, cortical-located lesion posteriorly to the corpus callosum (white void arrow). These lesions have a heterogeneous, mixed hypo- and hyperintense signal intensity with a reticular pattern and a peripheral hypo-intense rim. Perilesional edema and mass effect are absent. **Origin:** © Department of Radiology, Algemeen Ziekenhuis Sint-Maarten, Mechelen, Belgium, 2020

b

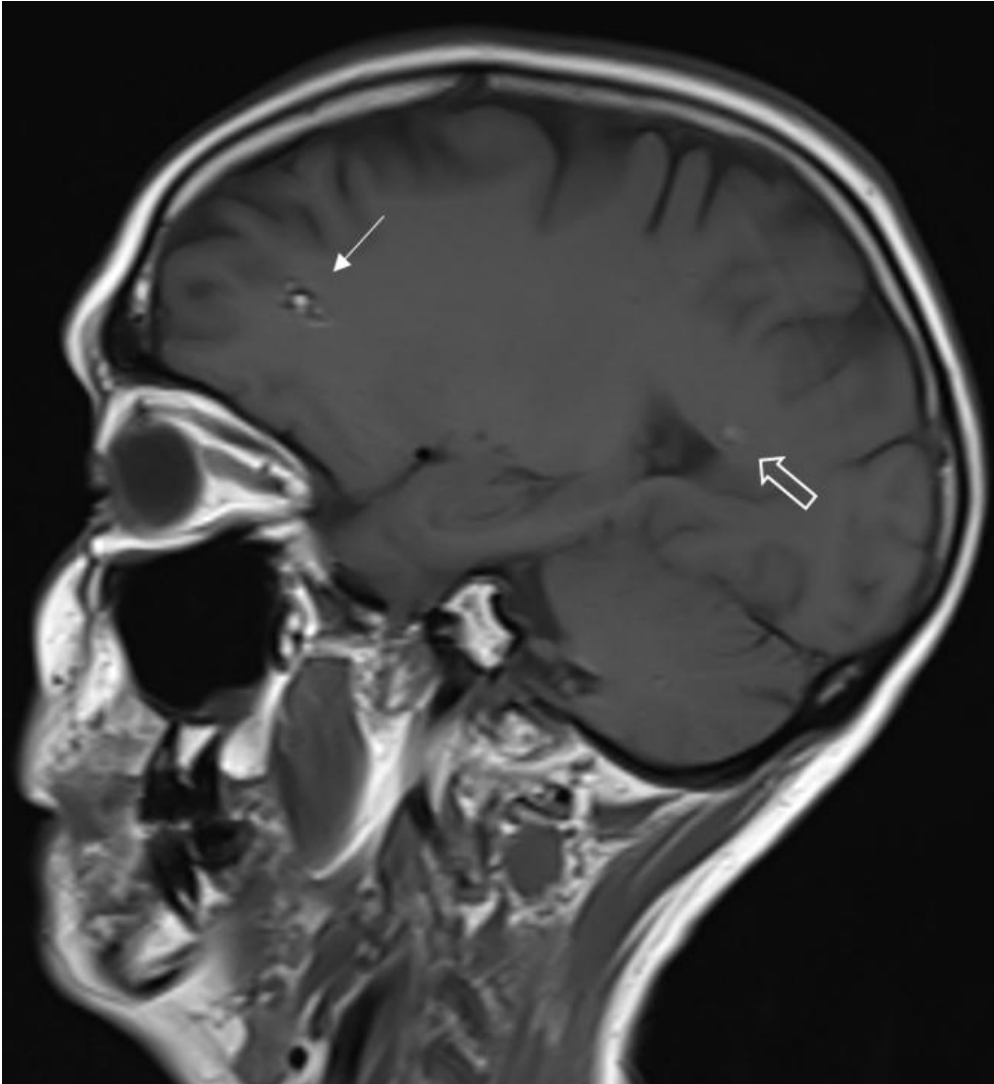


Description: FLAIR images confirm the heterogeneous, mixed hypo- and hyperintense subcortical-located lesions with a reticular pattern and a hypo-intense rim in the left frontal lobe (white arrow) and posteriorly to the corpus callosum (white void arrow). Perilesional edema and mass effect are absent.

Origin: © Department of Radiology, Algemeen Ziekenhuis Sint-Maarten, Mechelen, Belgium, 2020

Figure 5

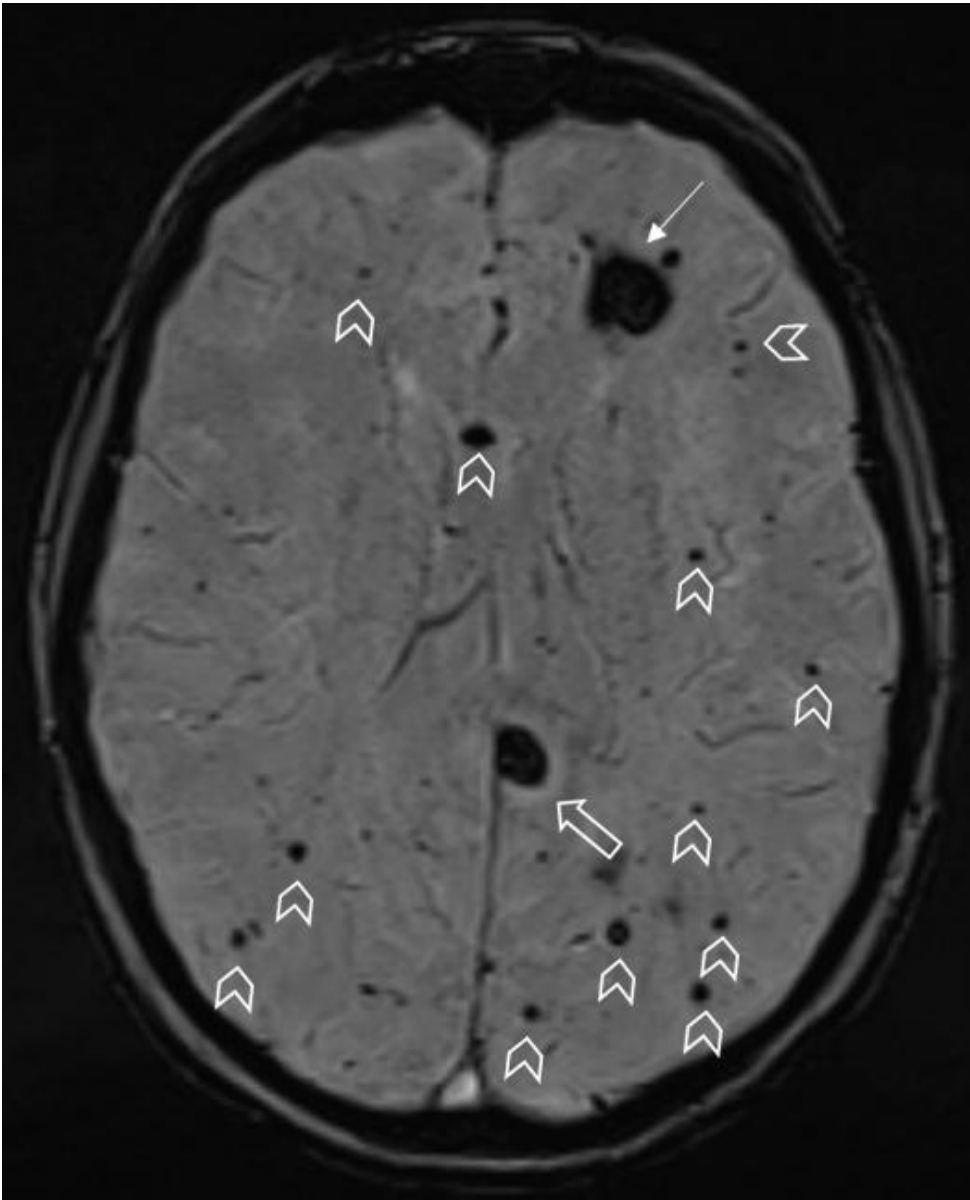
a



Description: Sagittal T1-WI shows mixed hyper- and hypo-intense signal in the subcortical-located lesion in the left frontal lobe (white arrow). The parafalcine lesion posteriorly to the corpus callosum is slightly hyperintense (white void arrow). **Origin:** © Department of Radiology, Algemeen Ziekenhuis Sint-Maarten, Mechelen, Belgium, 2020

Figure 6

a



Description: On SWI, there is marked blooming. Numerous additional hypo-intense, punctate lesions, not visible on other pulse sequences, are present (arrowheads). **Origin:** © Department of Radiology, Algemeen Ziekenhuis Sint-Maarten, Mechelen, Belgium, 2020